2010

Method for Quantitatively Analyzing Flow Phenomena in Annular-Mist Two-Phase Flows

Scott S. Wujek
University of Illinois at Urbana-Champaign

Predrag S. Hrnjak
University of Illinois at Urbana-Champaign

Method for Quantitatively Analyzing Flow Phenomena in Annular-Mist Two-Phase Flows

Scott. S. WUJEK*, Predrag S. HRNJAK

Department of Mechanical Science and Engineering
University of Illinois at Urbana-Champaign
Urbana, IL, USA
(Phone: (217)333-7706, E-mail: swujek@illinois.edu)

* Corresponding Author

ABSTRACT

A method has been developed which determines wave speed and wavelength of liquid flows on a tube surface. The features attributed to the surface flows are then removed in order to create an enhanced image of droplets in the focal plane of the camera. The method is described step-by-step and accompanied by resulting images. By knowing the length scale of the image, droplet size is calculated. Knowledge of the length scale and the framing rate of the camera, make it possible to determine the two-dimensional velocity field. Based on the amount of droplets in the enhanced image, an image analysis technique resembling PIV is utilized to determine droplet velocities.

The entire analysis technique has been automated allowing the analysis of 500 frames of video in roughly 3 hours. Knowledge of droplet size and velocity can be coupled with an understanding of droplet-film interactions to model droplet deposition.

1. INTRODUCTION

Annular-mist flows occur in high-quality, two-phase flows at relatively high mass fluxes. Commonly occurring in compressor suction and discharge lines in air-conditioning and refrigeration applications, annular-mist flows are formed by flowing refrigerant vapor and a liquid composed mostly of oil. A complete liquid annulus, rivulets, or droplets are manifest on the interior surface of the tube depending on the fluid properties and flow conditions. Visualization of flows within clear tubing is commonly performed with high speed cameras to gain insight of flow phenomena. Droplets, which make up the mist in the core of the flow, are obscured by the existence of liquid film, rivulets, or droplets attached to the tube wall.

Visualization in air-conditioning and refrigeration system components has been attempted by numerous researches in hopes of gaining fundamental insight of flow phenomena. Multiple phases facilitate this process because phase interfaces can be followed from frame to frame to understand the nature of the velocity field. Several papers from open literature have shown that fluids apart from refrigerant-oil combinations have been used to study flow inside refrigeration components. Srikanth and Thompson (1989) studied the flow a variety of suction mufflers and the intake manifold of a hermetic refrigeration compressor. Smoke, used to produce tracer particles, and air were drawn through a transparent muffler and a non-operational compressor by an auxiliary compressor. The flow patterns in the different muffler geometries were sketched by hand. Guerrato, *et al.* (2008) determined the velocity field in the discharge port and discharge cavity of a screw air compressor at one operating condition. They replaced part of the compressor housing with clear acrylic to allow the optical access necessary for laser Doppler velocimetry. The compressor was run without oil in order to keep the surfaces relatively clean, but atomized silicone oil was added for seeding particles. Many spatial regions of interest were used and thousands of measurements at each shaft angle were combined to formulate the velocity field. From these papers, it seems as though phenomena at the core of two-phase refrigerant-oil flow inside air-conditioning systems were not studied using the normal working fluid.

The main reason why researchers have resorted to using other fluids for tracking particles in air-conditioning systems is to avoid having a wavy liquid film build up on the visualization surface. Annular flow in straight tubes has been heavily studied by chemical and nuclear engineers researching two-phase flow in straight pipes. To study the movement of small entrained drops in the core of the flow while avoiding the problem of wavy film, the geometry of the pipe was modified. For instance, Hewitt and Whalley (1980) described the main optical methods used for determining properties in two phase flow, but also described a new visualization apparatus which allowed for a round tube to be viewed axially. By viewing the flow axially, instead of radially, annular flow did not obscure their vision. While standard filming could be used, a laser shadowgraph technique was shown to have a potential advantage of allowing the entire length of the tube to be visualized. Other researchers have removed the liquid film through a sintered metal section immediately upstream of the visualization location. Often when using sintered metal extraction sections, the sight glass was shielded from oil droplets by injecting pure gas between the sight glass and the core flow.

While these techniques allow for an unobstructed view of the core flow, they require modifying the geometry of the flow channel. If the interest is in studying the core flow within a specific geometry, it seems counter-intuitive to alter that geometry. It would be desirable if the only modification required to the component is to build it out of a transparent material.

The purpose of the method described in this paper is to allow droplets inside the annular core to be visualized inside any transparent component. The main innovation in the image analysis technique presented in this paper is the ability to diminish the appearance of large wavy structures caused by the wall film, while enhancing the appearance of droplets in the vapor core. Temporal and spatial determination of wavelength, wave speed, two-dimensional droplet velocity vectors, and droplet sizes can be automatically calculated using the method discussed.

2. OUTLINE OF METHOD

The first step in the process is to replace the component of interest with a transparent component of the same geometry. Next, the system is run, and the flow is recorded with a video camera. The video is converted to a matrix of numbers for analysis. The average intensity at each pixel in the frame over the course of the recording is calculated. The difference between the pixel values in each from and the average is then calculated. The fluctuation around the mean is used in the next stage of the analysis, where the wave speed is determined. After the wave speed is determined, the waves can be removed from each frame. This makes the droplets much more readily noticeable. Since not all artifacts of the waves from the original image can be completely removed, some sorting is necessary to determine which regions in the image are droplets. The size of droplets can be calculated from a single frame, and sequential frames are compared to determine droplet velocities.

3. TEST SETUP AND VIDEO RECORDING

The first step in the process is to replace the component of interest with a transparent component. While it is likely that surface properties, such as wetability and roughness, will not match those of the original component, the overall geometry of air-conditioning or refrigeration components can generally be replicated in clear glass or plastic.

As an example, images from laboratory testing will be used to demonstrate the image processing technique. In this example, the component of interest studied in the example was a discharge line. Besides providing fundamental understanding, these images may provide insight on improved oil separator designs. The system used for the example had a residential rotary compressor using R410A with polyvinylether (PVE) oil. Due to the relatively high temperatures and pressures associated with using this refrigerant and out of concern for vibrations, the discharge line was replaced by a transparent perfluoroalkoxy (PFA) tube. This material was found to be compatible with the refrigerant and oil. The tube had an inner diameter of 6.35 mm (1/4") and an outer diameter of 9.525 mm (3/8"). The tube was attached to the compressor using compression fittings.

Due to the high speed of droplets and waves in the annular film, a high speed Vision Research SR-CMOS camera was utilized to record images of the flow. This 8 bit black and white camera is capable of filming at 2000 frames per second at its full resolution, 512 by 512 pixels. Exposure times (shutter speeds) can be as small as 2 μs. Increased framing rate can be achieved at reduced resolution. The high framing rate and short exposure time allow

for individual droplets and waves to be tracked. Due to the relatively low resolution of the camera and the small size of most droplets, magnification from a microscopic lens improves the accuracy in determining droplet velocity and size. In this experiment, the microscopic lens system was produced by Navitar. The principle lens was a 5x objective from Mitutoyo. To determine the size of most of the droplets, the microscopic lens is set to its maximum zoom. The high speed video was recorded as close to the compressor as possible.

Due to short exposure times and high magnification, very intense light is required. The tube is backlit with a 150W fiber optic light source. When using the macroscopic lens, a translucent white diffuser is utilized. Due to the large aspect ratio of the tube and the small area being filmed at a given time, it is necessary to move the camera, lens, and light source to film the entire length of tube. A jig is used to precisely align the camera, lens, tube, and light source. The jig, along with the compressor and transparent discharge tube, can be seen in Figure 1.

Figure 1. Photograph of experimental facility utilized for example images

For the example video, 300 frames were recorded. Using a framing rate of 2000 frames per second, this video covered only 0.15 second of system operation. The raw images used as an example for demonstrating the image processing technique are shown in Figure 2. The center image, frame 2, is the image for which the technique will be demonstrated while the left and right images, frame 1 and 3 respectively, playing a role in understanding the central image. These images are arranged sequentially from left to right with the time elapsed between each frame being 454 microseconds. The fluid flows from right to left and gravity points to the right.

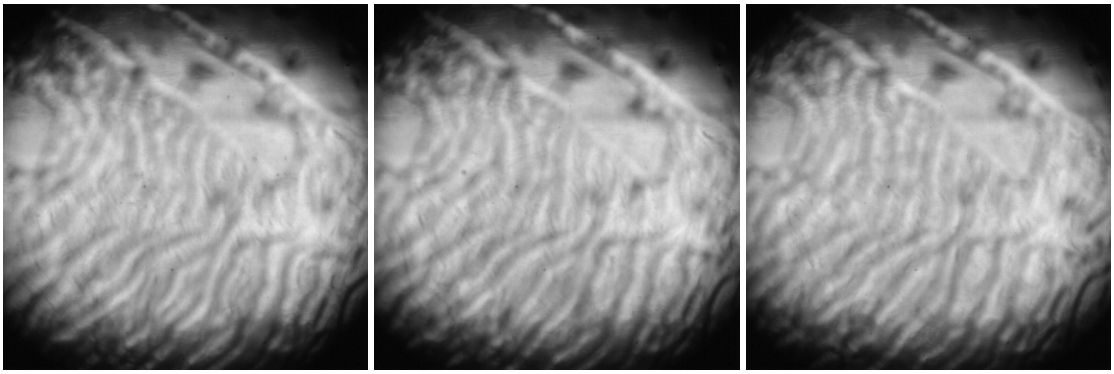

Frame 1 Frame2 Frame 3

Figure 2. Sequence of raw images used as an example

Once the video has been recorded, image analysis can begin. While MATLAB was used in conducting this analysis, any suitable computer programming language can be used. Due to the poor illumination of the image near the corners of the frame, the image was cropped slightly since little useful information can be collected in these regions. This helps to speed processing times by analyzing less overall information and decreasing computer memory usage per frame. Due to finite computer memory, and the number of operations required in processing the video, the entire sequence of 300 frames is divided into 3 sets consisting of 100 frames.

3. WAVE ELIMINATION

As a review of terminology, a frame is a two-dimensional image. Frames are recorded, and later shown, in sequence to create a video. Each frame is composed of dots, called pixels. Each pixel has a number, or pixel value, assigned to it. A pixel value relates to the amount of light which struck that pixel during the recording process and how white the pixel is when displayed. 0 corresponds to a completely black pixel, and 255 corresponds to a saturated, white pixel; shades of grey fall in between.

The primary mechanism by which waves in the central frame shown in Figure 2, will be eliminated comes from comparing features in one frame against those features found in the surrounding frames The first major step therefore, is to determine what each frame has in common. The average pixel value at a given location therefore is the arithmetic mean of the brightness of each pixel over all frames. The pixel values averaged over the entire example video are shown in Figure 3. Some features are readily apparent in this average frame. The light colored circle and dark corners are obvious. Large dark dots, likely formed by stationary oil on the tube wall can be seen. Some small specs which may be caused by tube imperfections, or dirt on the camera sensor, can also be noted.

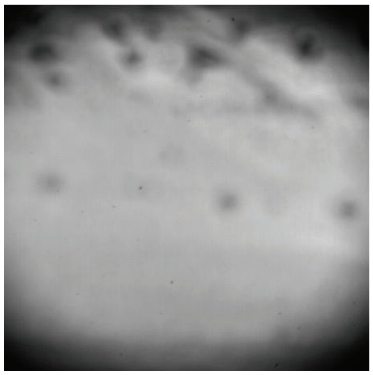

Figure 3. Average pixel values

The next step is to determine the fluctuation in pixel values from the average pixel values shown in Figure 3. The fluctuations are calculated by subtracting the average pixel values from the pixel values of each frame. As a result of this subtraction, some pixels are assigned negative values. Along with the subtraction process, the contrast is enhanced, particularly in darker regions to correct for uneven lighting. The results of the subtraction and contrast enhancement are shown in Figure 4. Since the subtraction would cause some pixel values to be negative, all pixel values have been increased by a 128, which is half way between completely black and completely white. The images seen in Figure 4 can be thought of as Figure 2 minus Figure 3 but with greater contrast.

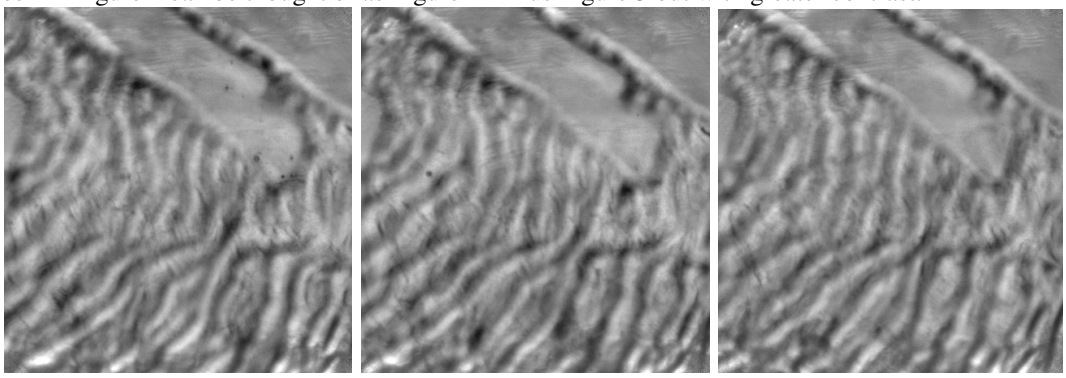

Frame 1 Frame2 Frame 3

Figure 4. Fluctuations from the average pixel values

After the images have been transformed into enhanced fluctuations from the mean, the waves in the film can be much more easily compared. Because the flow is from right to left in the frame, it can be rightly assumed that the

wave crests and troughs will also move to the left in each sequential frame. Pixel values taken from a single horizontal row, roughly ¾ of the way from the top of each of the three frame shown in Figure 4, have been plotted in Figure 5. The pixel values from a given frame appear to reassemble a saw-tooth wave. From the plot, it can be seen that the pixel values from each frame takes on a similar form. However, the positions of the waves are offset from one another, peaks and troughs from frame 1 appear to the right of those in frame 2. Likewise, the waveform given by frame 2 is to the right of frame 3. The size of the offset between the waves can be determined by calculating the cross-correlations between the pixel values taken from corresponding rows in sequential frames. Cross-correlations are mathematical computations where increasing values correspond to improved alignment. The location of the maximum in the cross-correlation corresponds to the displacement which must be applied to align two sets of signals as well as possible. The cross correlations for each row of the image is calculated. The median location of the maxima is used to determine the horizontal displacement of the wave in successive images. This technique finds the velocity of the waves, not of the small entrained droplets. The main reason for this is that the waves are much larger, more noticeable features than the small droplets. The offset between both frame 1 and frame 2 and between frame 2 and 3 were found to be 8 pixels.

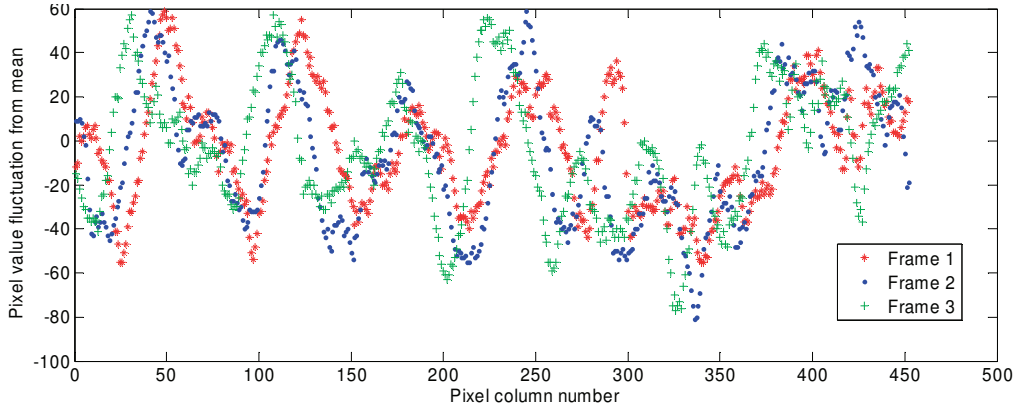

Figure 5. Pixel fluctuations from the 300th row from the three successive example images

By determining the frame to frame wave displacement, it is possible to remove most of the pixel fluctuations coming from the waves. Using the images shown in Figure 4, frame 1 and frame 3 are shifted by the displacement determined in the previous step to the left and right respectively to remove waves in frame 2. Since the waves are not steady, but instead grow, shrink, and merge, an assumption is made that pixel value fluctuations in frame 2 which are caused by the wave should generally fall between the pixel values at that same location in the shifted frames 1 and 3. If pixel values fluctuations in frame 2 are between the pixel value fluctuations from frame 1 and frame 3, the pixel value at that location will be set to zero. If the pixel value fluctuations in frame 2 are larger in magnitude than the fluctuations from frame 1 and frame 3, the closest pixel value from frame 1 or 3 is subtracted from frame 2. The results of this process for frame 2 are shown in Figure 6. As with Figure 4, the pixel values shown in Figure 6 have been increased by 128 in order to allow the information to be presented pictorially. In comparison to Figure 4, the droplet about halfway down the frame near the left side has become fare more noticeable and the waves are less noticeable.

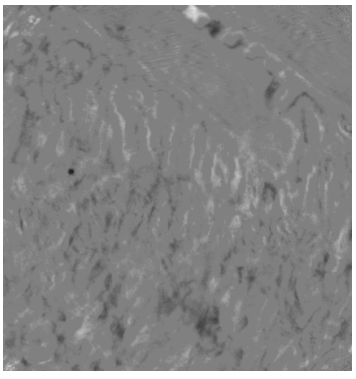

Figure 6. Frame 2 after first step in wave removal process

Some remnant of the wave is still seen in Figure 6, and appears as a white and black stripe pattern. Additional steps are implemented to remove this remnant while still retaining the pixel values corresponding to the droplet. Similar to the image processing used to transform Figure 2 to Figure 4, average pixel values are calculated. In this case however, the average only consists of the two previous and two subsequent frames. The moving average pixel value will be subtracted from the image shown in Figure 6. This moving average is especially useful in eliminating the effects of nearly stationary wave fronts that occur near the interface between dry and wetted walls. This interface tends to quickly oscillate between large and small pixel values as each wave joins this front. The results of this subtraction are shown in the left image shown in Figure 7. For this particular image only slight improvement is realized. Because there is some variance in the frame to frame displacement of each wave within the image, the extreme values used for subtracting fluctuations are now averaged over approximately 1/4 of the oil film wavelength. The results of this manipulation are shown in the right image in Figure 7. This results in a noticeable improvement in the regions of the image where the annular film was present.

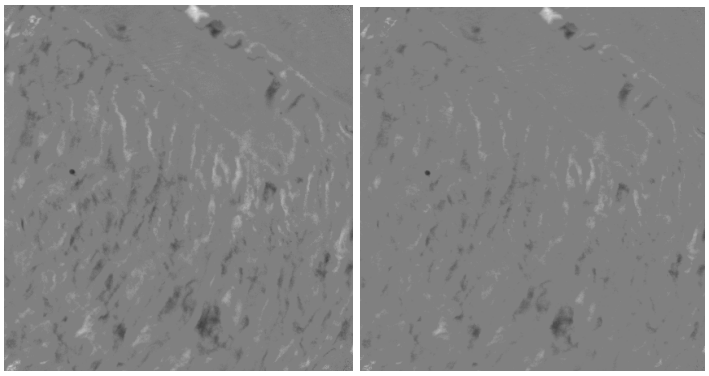

Figure 7. Frame 2 after (left) subtracting moving time average and (right) after accounting for non homogeneity in wave movement

Looking at the right image in Figure 7, there still remains some remnant of the wave. This is causing the striped pattern in the entire bottom half of the image. Some blotchiness in the image exists where the rivulet appeared near the top, right corner. Because the image was backlit in the filming process, droplets appear as dark regions. Refraction may cause the droplet to appear as a dark ring with a light core. Because droplets, which are the features of interest, appear as dark circular regions or rings, all light colored regions may be eliminated. This additional step yields the left image shown in Figure 8. This image is slight improvement because it eliminates some of the noise from the image.

To eliminate the remaining dark regions shown in the left image shown in Figure 8, another technique is utilized. Recalling the saw-tooth pattern shown in Figure 5, one can see that as the saw-tooth wave shifts from positive to negative values the slope remains constant. This continuous transition in pixel value fluctuations comes from the fact that the liquid wave surface is continuous. Droplets in a vapor core cause an optical discontinuity which means that the bright regions surrounding droplets see very minimal change in pixel value. In other words, the slope in pixel value fluctuations surrounding droplets has a very small magnitude. By extrapolating the slope in pixel value fluctuations from light regions into the dark regions, many of the remaining dark regions which are not due to droplets can be eliminated. The results after this stage in the wave elimination sequence are shown in the right portion of Figure 8. While many of the dark regions remain, in most cases they are smaller and lighter than before while the droplets appear nearly as dark as before.

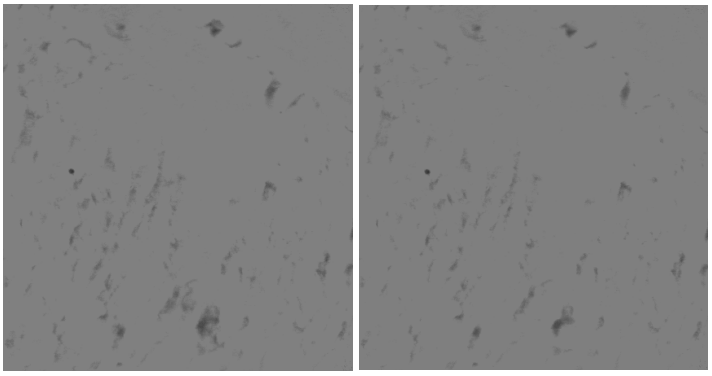

Figure 8. Frame 2 after additional processing (left) bright regions also removed (right) dark portions of waves also removed by slope extrapolation

3. DROPLET DETECTION

From this point forward, analysis will be conducted on the individual dark regions instead of on the frame as a whole. The first step in analyzing the dark regions is to determine what is considered to be a dark region. This is done be setting a pixel value threshold where only regions darker than the threshold will be considered as dark regions. This threshold value is determined by the pixel value noise, as determined by the standard deviation of the improved images. To make regions more continuous, morphological operations, such as filling holes in the dark regions and bridging unconnected pixels, are performed. The dark regions can be seen in the left side of Figure 9; a border has been added to aid the reader.

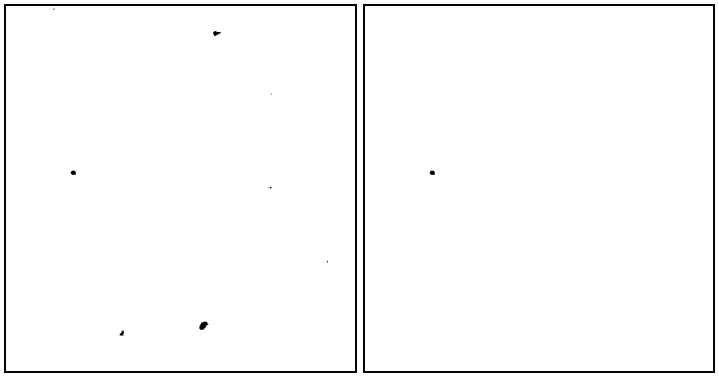

Figure 9. (left) Frame 2 dark regions; (right) Frame 2 final droplet determination

Each dark region is now analyzed to sort droplets from dark regions caused by waves. Because waves are continuous it is intuitive to look at the pixel values surrounding the dark region. To do this, the size and location of each dark region is determined. The average fluctuation pixel value in the location of the dark region is calculated. Adjoining regions, in the four cardinal directions, having the same size and shape as the dark region are selected. The average fluctuation pixel value in each of the four regions is determined. For a dark region to be sorted into the droplet category, and not as part of a wave, it must be noticeably darker than the surrounding regions. While this eliminates the vast majority of dark regions not caused by droplets, the aspect ratio of the dark region has also been found to relate dark regions to droplets. The final result is shown in Figure 9. Only one droplet was found in frame 2, which agrees well with results from personal observation.

4. DROPLET SIZE AND SPEED CALCULATION

Images, like the final image shown in Figure 9, can now be used to determined droplet size and speed. For a given magnification, it is possible to scale the size of the dark region to the physical size of the droplet. Although the size

of the droplet may be estimated directly from the size of the dark regions shown in the figure, this threshold based technique is extremely subjective in determining droplet size since different threshold values modify the calculated droplet size. For this reason a different method is preferred. One benefit of the preferred method is that it determines only the size of droplets which are in focus. Once the droplets locations are identified, droplet size is determined by reverting back to the pixel value fluctuations shown in Figure 4. The "half-height" is the average of the darkest pixel region and the background noise surrounding the region. The gradient in pixel values at the pixel closest to the half-height is determined in each of the four cardinal directions from the centroid of the dark region. If the gradient in pixel values exceeds the gradient required to be considered in focus, the size of the droplet is determined by averaging the distance between both the vertical and horizontal half-heights. While this method is still subjective in deciding what gradient is necessary for a droplet to be considered in focus, it does not systematically skew the droplet size distribution. This basis for this method was developed by Hay (1998). For the droplet shown in the example frame, the diameter was found to be 66 micrometers.

To determine velocity, the same droplet must appear in consecutive frames. Velocity vectors for the droplets may be calculated using an image processing technique similar to that used in two-image particle image velocimetry (PIV). Velocity vectors are determined using two-dimensional cross correlations. PIV type analysis has the advantage of determining the velocity field over a relatively large area, not just at an arbitrarily small location. When cross-correlations are computed using the final droplet determination images, like that shown in Figure 9, spatial accuracy is the size of a single pixel.

5. CONCLUSIONS

An image processing technique was shown to successfully isolate droplets seen in annular two-phase, refrigerant-oil flow. As part of this processing technique the velocity of waves in the annular film is determined. The primary advantage of this image processing technique is to allow information about the droplets in the core of the flow to be easily extracted from the complex images produced by annular flow. Because of this procedure, it is unnecessary to modify a component in any way besides constructing it from transparent material to allow visualization. Once the droplets have been found, existing techniques for determining droplet size and speed may be utilized.

REFERENCES

Hay, H. J., Liu, Z., & Hanratty, T. J. 1998, A backlighted imaging technique for particle size measurements in two-phase flows: Experiments in Fluids, 25, 226-232.

Hewitt, G. F. & Whalley, P. B. 1980, Advanced optical instrumentation methods: International Journal of Multiphase Flow, 6, 139-156.

Guerrato, D., Nouri, J. M., Ntosic, N., Arcoumanis, C., and Smith, I. K. 2008, Flow measurements in the discharge port of a screw compressor, Proceedings of the IMechE, 222 Part E: Journal of Process Mechanical Engineering, 201-210.

Srikanth, R. & Thompson, H. D. 1989, Flow visualization applied to a small refrigeration compressor: International Journal of Refrigeration, 13, 7-12.

ACKNOWLEDGEMENT

The authors are thankful to the member companies of the Air-Conditioning and Refrigeration Center at the University of Illinois at Urbana-Champaign for their continued support.